Ionic Liquids in Electrochemistry

Subjects: Electrochemistry
Contributor: Ana Ribeiro

The roles of room temperature ionic liquids (RTILs) and RTIL based solvent systems as proposed alternatives for conventional organic electrolyte solutions are described. Ionic liquids are introduced as well as the relevant properties for their use in electrochemistry (reduction of ohmic losses), such as diffusive molecular motion and ionic conductivity.

Keywords: ionic liquid ; electrochemistry

1. Introduction

Working safety is nowadays considered a more important issue than performance, and the delivery of safe and efficient materials for practical uses has been taken into account in the research and development (R&D) efforts. Thus, new features in materials are expected to appear in the immediate future, aiming to boost the transition to greener technologies towards meeting the goals of the 2030 EU Agenda for Sustainable Development [1] and resolving the ambitious challenges endorsed by the EU 2050 Green Deal [2]. Room temperature ionic liquids (RTILs), or simply ionic liquids (ILs), are an example of this new type of development, providing solutions for practical applications [3][4][5].

Ionic liquids are (mainly organic) salts exhibiting a very low melting temperature (liquids below 100 °C) and extremely low (negligible) vapor pressure [4]. Lately, they have received significant attention from the scientific community due to such unusual properties as liquids, being considered as suitable substitutes for volatile organic solvents (VOC, one of the major sources of waste in chemical synthesis) [6]. In fact, due to the unique physicochemical properties of ionic liquids the last decade has seen a remarkable boost on their application in several fields (e.g., chemistry, materials science or chemical engineering) with a significant high number of scientific contributions (ca. 68,057 publications in the period November 2010–2020, Figure 1).

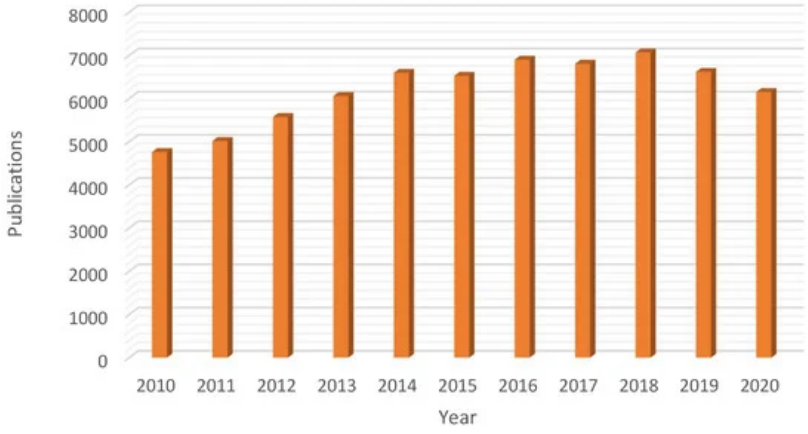

Figure 1. Rising interest on the use of ionic liquids: yearly number of publications in the domain of ionic liquids in the 2010–2020 period (Database: Scopus, search terms: “ionic” AND “liquids”, search date: 7 November 2020).

Room temperature ionic liquids general physicochemical properties are summarized in Table 1.

Table 1. General characteristics of room temperature ionic liquids [7].

General Properties	Features

Low melting point	• Treated as liquid at ambient temperature • Wide temperature interval for applications
Non volatility	•Thermal stability • Flame retardancy
Composed by ions	• High ion density • High ion conductivity
Organic ions	• Designable/Tuneable • Unlimited combinations possible

Clearly, the physicochemical properties presented in Table 1 for RTILs are very different from those exhibited by ordinary molecular liquids. However, it is worth mentioning that every ionic liquid does not always show the above properties.

Ionic liquids are almost all times composed of organic ions, and therefore have unlimited structural variations in view of the easy preparation of many different components. The tuneability of combinations of cations and anions and the possibility to achieve modifications of the cation and/or the anion part offer access to ionic liquids with targeted properties. This has led to an exponential expansion of the number of multipurpose, interesting ILs known in recent years. Some of the most common ionic liquids components (cations and anions) are presented in Table 2.

Table 2. Structures of most common ions used in designing ionic liquids. Adapted, with permission of ref. [5], copyright, 2020, Elsevier.

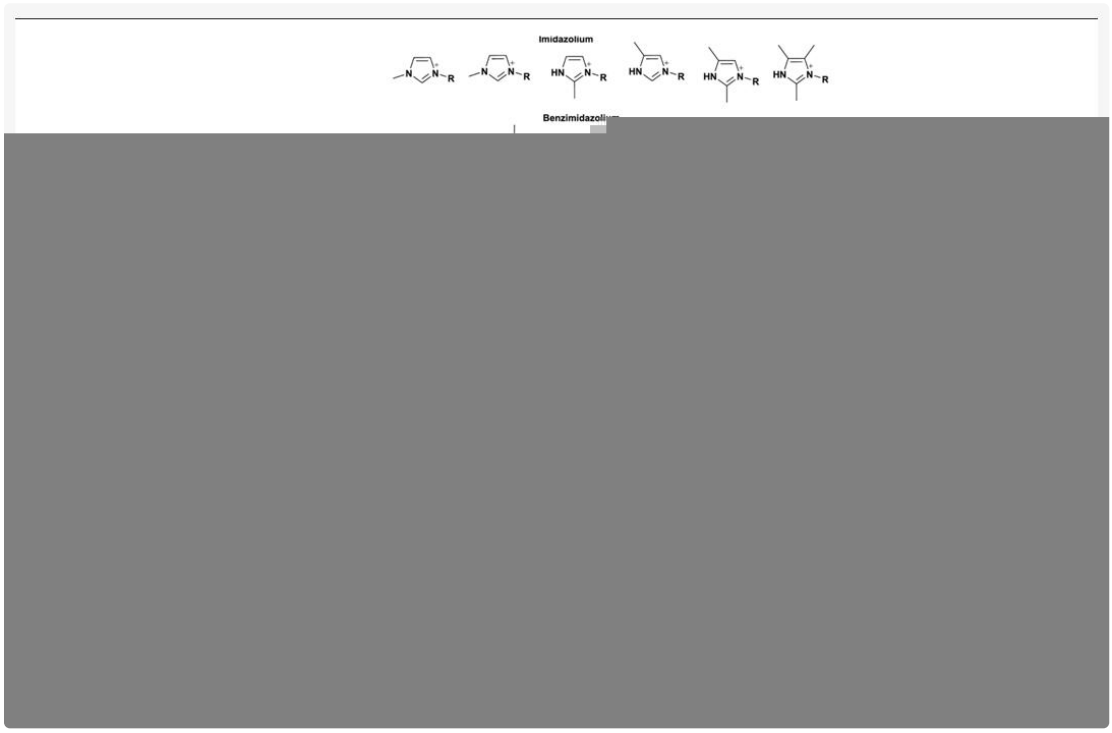

Imidazolium-based ILs, such as 1–butyl–3–methyl–imidazolium [bmim] and 1–ethyl–3–methyl–imidazolium [emim], are among the most studied due to their stability within oxidative and reductive conditions, low viscosity, and ease of synthesis [8]. The cationic component of ILs has been varied to include pyridinium, ammonium, phosphonium, thiazolium, and triazolium species [5] (Table 2). In general, these cations have been combined with weakly coordinating anions, although not all weakly coordinating anions result in ILs [9]. Common examples include tetrafluoroborate, hexafluorophosphate, triflate, triflimide, and dicyanamide (Table 2). The first two have been explored the most and must be treated with the greatest caution as they are fairly readily hydrolysed to boric acid and phosphate, respectively [4]. Indeed, various phosphate and phosphinate anions (Table 2) have been employed bearing some advantages in RTILs [4][5].

Different potential applications of ionic liquids rely on their physicochemical properties, which vary based on the structures of the cation and anion used to assemble them (Table 2). A general understanding of these properties requires a detailed understanding of ionic liquid at the molecular level, namely the anion–cation interactions, which has been addressed in

several previous reviews [5][10].

For instance, the ILs flame retardancy, based on the non-volatility inherent to ion conductive liquids, opens up the possibility for their application in the energy sector. In fact, ionic liquids are being developed for energy devices that need to use safe materials (avoiding accidental explosion or ignition) [7].

For electrochemical usage, the most important properties should be both electroconductivity and ion conductivity [11]. These are essentially the properties of advanced (and safe) electrolyte solutions that are critical to energy devices. For example, currently, electrochemical capacitors are limited in the cell voltage [12] due to the degradation of the applied electrolytes, based on organic solvents. Since the storable energy and power are dependent on the square of the cell voltage, it is worth investing in (safer) alternatives to the state-of-the-art electrolytes.

Electrolytes should have high ionic conductivity to minimize ohmic losses, high salt concentration to prevent starvation effects, a high electrochemical stability window in an appropriate temperature range, as well as high safety and low environmental impact.

Aqueous electrolytes exhibit very high ionic conductivities. However, their electrochemical stability window is very limited (the thermodynamic stability of water, at room temperature, is 1.23 V [13]), and therefore are not suitable to use at a wide temperature range or on a very small scale (due to the 100 °C boiling point of water) and are usually highly corrosive.

Non-aqueous common electrolytes (e.g., tetraethylammonium or triethylmethylammonium tetrafluoroborate salts in acetonitrile) also display very limited potential windows mainly due to the decomposition of the used solvent (e.g., the potential window of commercially available devices based on acetonitrile is 2.7 V [14]).

The use of ionic liquids as solvent free electrolytes might be one way to overcome the above potential window limitations. In fact, RTILs often display larger electrochemical stability windows (Table 3) [15][16] as compared to common non–aqueous electrolytes, concomitant with high thermal stability, non-flammability and in certain cases high conductivity.

RTILs exhibit a broad range of conductivities spanning from 0.1 to 20 mS cm^{-1} [17]. In general, higher conductivities are found for imidazolium based ILs in comparison with the ammonium ones. Many factors can affect their conductivity, such as viscosity, density, ion size, anionic charge delocalization, aggregations and ionic motions [18]. Strong ion-pair associations have been invoked in the case of bis(trifluoromethylsulfonyl)imide ($[NTf_2]^-$, Tf = triflate) based ILs, to understand their lower conductivity in comparison with tetrafluoroborate based ionic liquids [18].

The applicable electrochemical potential window of ILs can be determined using well-known electrochemical methods, such as cyclic voltammetry, and is typically found to be similar to or slightly larger than that found in conventional organic solvents, but much larger than that of aqueous electrolytes (Table 3). Imidazolium-based ILs display shorter electrochemical windows than the phosphonium ones indicating a higher electrochemical activity of the formers. In fact, by reduction, imidazolium ion can lead to the formation of N-heterocyclic carbenes [19]. Thus, the challenge is to design RTILs with a wide electrochemical window along with good electrical conductivity.

Table 3. Examples of electrochemical potential window of selected phosphonium- and imidazolium-based ionic liquids and standard aqueous and non-aqueous electrolytes.

IL [a]	Solvent	Salt	Electrode	Potential Window/V	Reference

$[P_{2225}][NTf_2]$				6.3	
$[P_{2228}][NTf_2]$				6.4	
$[P_{222(1O1)}][NTf_2]$				5.7	[15]
$[P_{222(2O1)}][NTf_2]$			Pt wire	5.4	
$[bmim][NTf_2]$	-	-		3	[16]
$[bmim][NO_3]$			Carbon film	2.8	
$[Pyr_{14}][NTf_2]$			TiC-CDC	2.5	[20]
$[Pyr_{14}][NTf_2]$			AC	3.5	[21]
$[EdMPN][NTf_2]$			Sucrose	± 2.3	[22]
-	Acetone	$[NEt_4][ClO_4]$, $[NBu_4][PF_6]$, $NaClO_4$	Pt wire	3.5	[23]
	CH_3CN	$[NEt_4][ClO_4]$, $[NBu_4][PF_6]$, $LiClO_4$		4	
	CH_2Cl_2	$[NBu_4][PF_6]$, $[NBu_4][ClO_4]$, $[NBu_4][X]$ (X = Cl, Br, F, I)		3.7	
	DMF	$[NEt_4][ClO_4]$, $[NBu_4][PF_6]$, LiCl, $NaClO_4$		4.3	
	DMSO	$[NEt_4][ClO_4]$, $[NBu_4][PF_6]$		3.3	
	THF	$[NBu_4][PF_6]$, $LiClO_4$, $NaClO_4$		3.7	
	H_2O	$NaClO_4$, KNO_3		2	

$[P_{2225}][NTf_2]$ = triethyl-n-pentylphosphonium bis(trifluoromethylsulfonyl)amide; $[P_{222(1O1)}][NTf_2]$ = triethyl(methoxymethyl)phosphonium bis(trifluoromethylsulfonyl)amide; $[bmim][NTf_2]$ = 1-butyl-3 methylimidazolium bis(trifluoromethylsulfonyl)imide; $[Pyr_{14}][NTf_2]$ = 1-butyl-1-methylpyrrolidinium bis(trifluoromethanesulfonyl)imide; $[EdMPN][NTf_2]$ = ethyldimethylpropylammonium bis(trifluoromethylsulfonyl) imide.

Therefore, ionic liquids having a large electrochemical potential window and particularly unique physicochemical properties (e.g., negligibly small vapor pressure), constitute promising (and safer) candidates for the substitution of currently used electrolyte solutions based on organic molecular solvents. They have been applied as media for electrodeposition of metals [24], electrochemical biosensors [25], supercapacitors [26][27], batteries [28][29], and solar cells [30][31].

2. Imidazolium-Based Ionic Liquids

The imidazolium based ILs constitute the class of ionic liquids most used in electrochemical applications. The ones bearing two to four carbon atoms in the cation chain length, such as 1–butyl–3–methyl–imidazolium [bmim] or 1–ethyl–3–methyl–imidazolium [emim], respectively, are preferred, namely for electrodeposition processes.

Caporali et al. applied 1–Butyl–3–methyl–imidazolium bis(trifluoromethylsulfonyl)imide, [bmim][NTf_2] (Tf = triflate) for the electrodeposition of a group of transition metals, such as silver, copper, cobalt, nickel, or zinc [32]. The metal was dissolved in such IL, under conditions suitable for industrial applications, i.e., an uncontrolled (moisture content) atmosphere, and electrochemically characterized by cyclic voltammetry and chronoamperometry.

Silver was present in [bmim][NTf_2] in the form of uncoordinated or weakly coordinated Ag^+ ions, and therefore represented the simplest electrochemical system. Homogeneous and crack-free silver coatings were potentiostatically obtained from this ionic liquid. The authors used a “dry” and a “wet” sample, were the water content was determined by Karl Fischer titration. The electroreduction of Ag^+ was favoured in the “wet” system, but in both cases the reverse sweep showed a current crossover and a reduction peak that was dependent on the scan rate. Moreover, when they increased the scan rate, the peak potential value moved towards more negative values. Both of these observations are indicative that silver electroreduction follows a nucleation-growth mechanism. Thus, chronoamperometric measurements were carried out by stepwise variations of the potential of the working electrode from a value where no reduction of silver occurs to potentials sufficiently negative to induce the reduction process. In this manner, the electro-crystallization mechanism, by comparing experimental data with calculated values obtained from a theoretical model, was determined by the authors, that also compared their observations with previous published results obtained using other types of ionic liquids. They concluded that, in the “wet” system, the overpotential required to start the electroreduction is lower and the maximum current value is higher. This phenomenon was partially attributed to the enhanced Ag^+ ion mobility due to the decreased viscosity of the electrochemical medium resulting from the presence of a larger amount of water. In the dry system, probably due to the lower mobility of the electroactive species, the effect of overpotential is less marked.

In contrast, copper-, cobalt-, and zinc-bearing systems were highly moisture sensitive. The majority of these metals were reduced at atmospheric pressure and at a scan rate of 100 $mV.s^{-1}$. The authors pointed out that the addition of the metal salts to the hydrophobic [bmim][NTf_2] considerably increases the ability of this IL to absorb water from the atmosphere and, therefore, the mild dehydrating experimental conditions employed assured only partial water removal. Therefore, the voltammogram recorded in the “dry” and “wet” system could not be directly compared, leading to a determination of the growth mechanism only in the “wet” systems. The authors concluded that the presence of large amounts of water changed the nature of the coordination species present in the solution, facilitating the electroreduction of the metal centres, and had also effects on the displayed colours of the samples. Nevertheless, metallic deposits were obtained, and their morphologies investigated as a function of the deposition potential and water content. Only in the case of the Ni-bearing IL did the authors report that it didn’t form electroactive species.

In this study, Caporali et al. [32] used very simple operating conditions that did not require a rigorously controlled atmosphere. This advantage made the process particularly easy for a potential upgrading for large low-cost applications.

The IL 1-butyl-3-methyl-imidazolium chloride, [bmim]Cl, was used as electrolyte in the study of the redox properties of Cu(I) and Cu(II) ions, showing that the Cu(I) ion can be oxidized to Cu(II) and reduced to Cu(0), and that Cu(II) can be reduced to Cu(I) by the metallic Cu(0) [33]. These electrochemical processes are depicted in Figure 2.

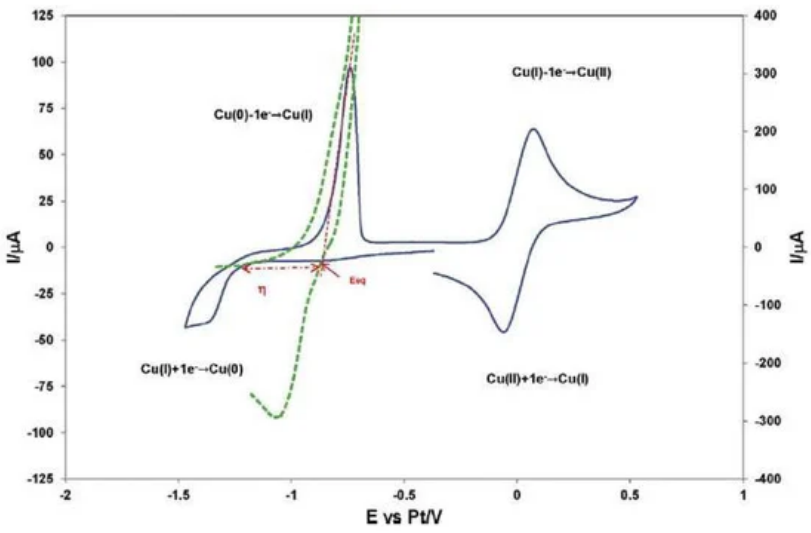

Figure 2. Cyclic voltammogram for Cu deposition on a Pt electrode exhibiting a nucleation overpotential (green); Cyclic voltammogram obtained on a Pt electrode in the [bmim]Cl without Cu(I) (blue). Reproduced with permission from [33], copyright 2016, Elsevier.

According to the authors, the experimental voltammograms suggested the presence of a nucleation phenomenon (Figure 2), but mainly in a qualitative way. The electrodeposition of copper occurs, and the explanation given is that the formation of stable Cu nuclei on an inert surface requires a potential more negative than the reduction of Cu(I) on a copper surface. Chronoamperometry was also performed to understand the nucleation/growth process of copper on a Pt wire and a Pt disc electrode.

The applications of rare earth metals in technological devices such as cell phones, and other electronic devices, as well as in permanent magnets leads to a pressing need to find a way to recycle them.

Gupta et al. [34], studied, by cyclic voltammetry and chronoamperometry at a glassy carbon electrode, the electrochemical properties of europium(III) aiming at to understand the oxidation state, coordination geometry, and physicochemical behaviour of the Eu(III) complex bearing di-hexyl-*N*,*N*-diethylcarbamoylmethylphosphonate (DHDECMP) ligand (as complexing extractant) in [bmim][NTf_2]. The reduction of Eu(III) to Eu(II) in [bmim][NTf_2] has shown a quasi-reversible reduction, at a peak potential of −1.44 V vs. Fc/Fc^+ (Fc = ferrocene), and was controlled by diffusion and charge transfer kinetics (Figure 3).

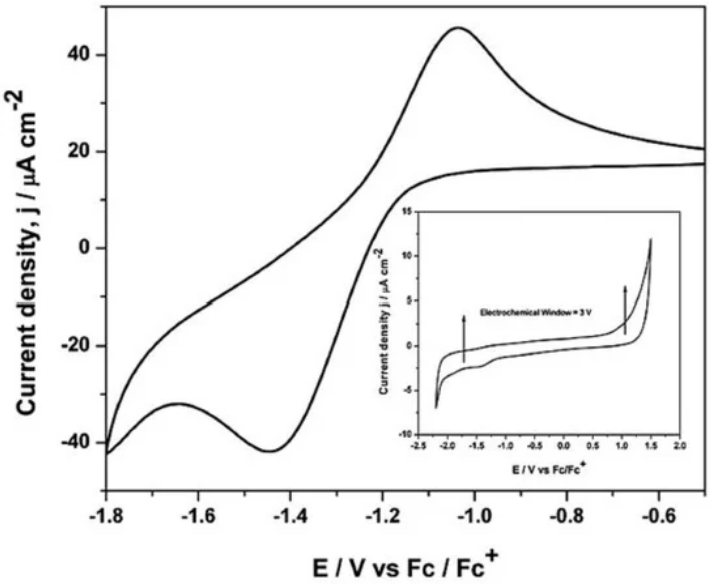

Figure 3. Cyclic voltammogram of 50 mM Eu(III) ions in [bmim][NTf_2] at 20mV/s. Inset: Cyclic voltammogram of [bmim][NTf_2] at a glassy carbon electrode at 25 °C. Reproduced with permission from [34], copyright 2015, Wiley.

The cyclic voltammogram of [bmim][NTf_2], recorded at a glassy carbon working electrode, is shown in the inset of Figure 3. The reduction of the $[bmim]^+$ cation occurs at a potential of −2.0 V (vs. Fc/Fc^+), and the oxidation of the $[NTf_2]^-$ anion occurs at 1.0 V (vs. Fc/Fc^+), allowing to detect the reduction of Eu(III) to Eu(II). Photoluminescence spectroscopy confirmed that the symmetry around the europium ions at Eu^{3+}–DHDECMP in the [bmim][NTf_2] was relatively low. By fluorescence lifetime measurements, the authors also determined that the number of water molecules in the inner sphere is six for non-complexed europium ions, and practically no water molecules was retained in the presence of the complexing extractant DHDECMP.

An IL with a higher cation chain length, [hmim][NTf_2] (hmim = 1–hexyl–3–methyl–imidazolium), was applied in the study of the redox properties of europium(III) for the recovery of europium by an extraction–electrodeposition (EX-EL) procedure [35]. The cyclic voltammogram of Eu(III) in [hmim][NTf_2], recorded at a glassy carbon electrode, exhibited a prominent quasi-reversible reduction wave occurring at the onset of −0.25 V vs. Fc/Fc^+ (Fc = ferrocene), culminating in a peak at −0.84 V vs. Fc/Fc^+ assigned to the reduction of Eu(III) to Eu(II), as shown in Figure 4.

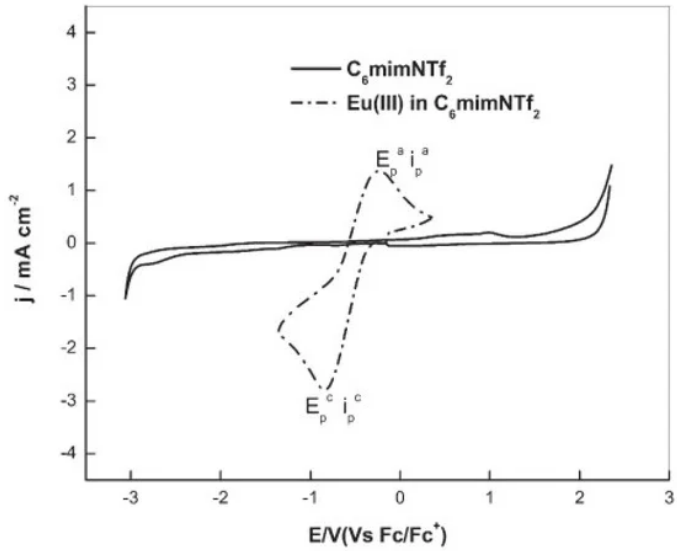

Figure 4. Cyclic voltammetry of [hmim][NTf_2] (—) and Eu(III) in [hmim][NTf_2] (----) recorded at glassy carbon electrode. [Eu(III)] = 100 mM, scan rate = 100 mV/s, T = 373 K. Reproduced with permission of ref. [35], copyright, 2015, Springer.

The cathodic peak current was lowered, and the peak potential shifted cathodically in the presence of tri-n-butyl phosphate (TBP) and N,N-dihexyloctanamide (DHOA) as ligands, due to the co-ordination of Eu(III) to such species in the ionic liquid medium (Figure 5). Moreover, the presence of TBP in the ionic liquid medium shifts the Eu(III) to Eu(II) peak potential to more negative values as compared to DHOA (compare Figure 5A,B).

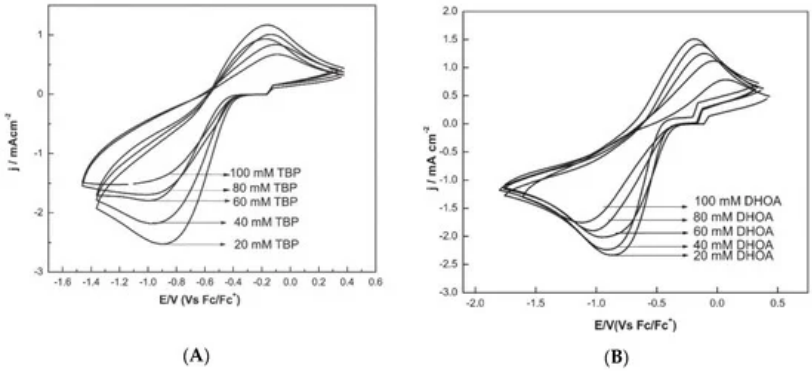

Figure 5. Cyclic voltammograms of Eu(III) (100 mM) recorded at glassy carbon electrode at a scan rate of 100 mV s^{-1} and at 373 K, in (**A**) TBP/[hmim][NTf_2] or (**B**) in DHOA/[hmim][NTf_2]. Reproduced with permission of ref. [35], copyright, 2015, Springer.

The stability constants of Eu(III)–ligand complex showed that the stability of Eu-DHOA complex in ionic liquid medium was lower than that of the Eu-TBP complex, and therefore the use of DHOA ligand for facilitating the electrodeposition of europium from the ionic liquid during the recovery of europium by extraction–electrodeposition (EX-EL) procedure would be the best option.

Krishna et al. [36], attached the neutral ligand DHOA to [bmim][NTf_2] to study the electrodeposition of a series of lanthanides (Ln), such as europium, neodymium, or dysprosium. The reduction of Eu^{3+}, Nd^{3+}, and Dy^{3+} to their respective metallic forms was successfully achieved (Figure 6).

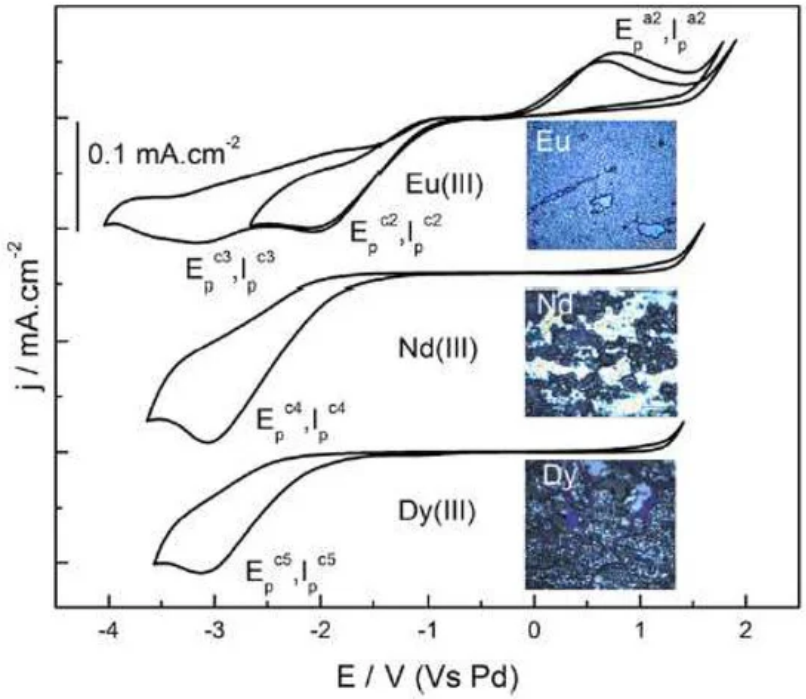

Figure 6. Cyclic voltammograms of 100 mM [Ln(NTf_2)$_3$] in DHOA medium recorded at glassy carbon working electrode at the scan rate of 50 mVs^{-1} at 353 K. Insets show the photographs of the electrodeposits obtained at the working electrode after electrolysis of 100 mM Ln^{3+} in the system DHOA/[bmim][NTf_2] at −3.0 V for about 2 h. Reproduced with permission from [36], copyright 2020, Elsevier.

To enhance their solubility, the investigation of the electrochemical behaviour of the lanthanide(III) ion present in neutral ligand-ionic liquid (NLIL) was performed by cyclic voltammetry. Figure 6 shows that the there is a two-step reduction observed for Eu^{3+}, whereas the NLIL containing Nd^{3+} and Dy^{3+} underwent a single step 3-electron transfer reduction at the cathodic potential of −3.0 V. The authors also confirmed that the anodic waves, corresponding to the oxidation of Nd^0 or Dy^0 to higher oxidation states, were not observed during the performed reversed scans.

Sengupta et al., [37] used [bmim][NTf_2] *to report* a first-ever cyclic voltammetric electrochemical characterization of *neptunium(IV)* complexes bearing the diglycolamide ligand. Np(IV) was found to undergo mono-electron exchange reactions. The activation energy values were deduced using the Arrhenius equation and thermodynamic parameters were derived using linear regression of the data. The redox reactions of the Np(IV) complexes were exothermic. In a further study, the authors [38] detected, by cyclic voltammetry, a different electrochemical behaviour for *neptunium(IV) bearing* diphenyl-N,N-diisobutylcarbamoyl-methylphosphine oxide *in [bmim][NTf_2]* (CMPO-*NTf_2*): for the redox couples involving complexes of Np(IV) with CMPO or CMPO-*NTf_2*, the enthalpy values were positive or endothermic.

Later, Rama et al., [39] used [bmim][NTf_2] to investigate the electrochemistry performance of U(VI). The cyclic voltammogram of U(VI) in *[bmim][NTf_2],* recorded at a glassy carbon working electrode at the scan rate of 100 mV/s at 373 K, exhibited a prominent *quasi-reversible reduction of U(VI) to U(V) (Figure 7), where the* cathodic peak potential was shifted anodically and the cathodic peak current increased with the increase of temperature. *The presence of tri-n-octyl phosphate* (TOP) *or tri-n-butyl phosphate* (TBP, a reference extractant) *ligands shifted the cathodic peak to more negative potentials due to the formation of a U(VI) complex (compare Figure 7A,B).*

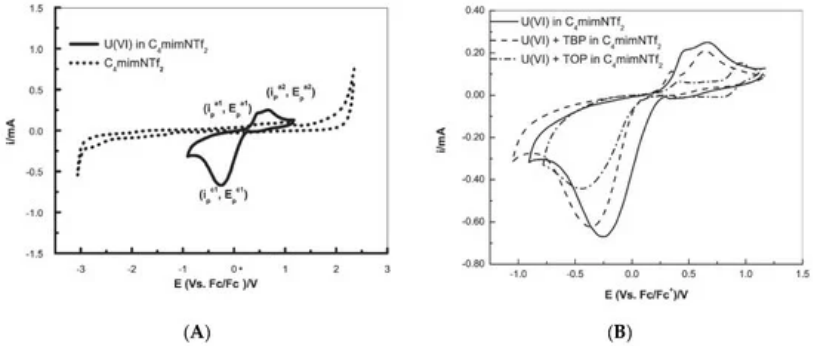

Figure 7. Cyclic voltammograms recorded at a glassy carbon electrode ([U(VI)] = 100 mM, scan rate = 100 mVs^{-1}, T = 373 K) of (**A**) [bmim][NTf_2] (----) and U(VI) in [bmim][NTf_2] (—); and (**B**) U(VI) in [bmim][NTf_2], in TBP/[bmim][NTf_2] and in TOP/[bmim][NTf_2]. Reproduced with permission from [39], copyright 2016, Elsevier.

One year later, Krishna' group extended the study of the redox properties of U(VI) by using [bmim][Cl], which increased the cathodic current density and consequently the U(VI) reduction was facilitated [40].

The above work was followed by the use of imidazolium-based IL bearing the dicyanamide anion [bmim][DCA], by the same researchers [41], to study the electrochemical behaviour of UO_2^{2+}. The cathodic peaks corresponding to the reduction of UO_2^{2+} to UO_2^{+} and then to UO_2 were clearly detected, indicating that [bmim][DCA] is a good solvent for this lanthanide cation.

Aiming at to accelerate the energy transition (urgent to be adopted in order to reduce anthropogenic causes for climate changes), an intense research is being developed in electrochemical processes of energy conversion and storage, through the design of new materials, namely ionic liquids, which would be able to increase the energetic efficiency of important processes.

The suitability of room temperature ionic liquids as solvents for redox flow batteries (RFBs) containing metal complexes was investigated by Ejigu et al. [42], using metal acetylacetonate (acac) complexes [$M(acac)_3$], (M = Mn, Cr, or V) in imidazolium based RTILs. They detected, by cyclic voltammetry at a glassy carbon electrode, an irreversible behaviour for [$Mn(acac)_3$] and [$Cr(acac)_3$] in 1-ethyl-3-methylimidazolium bis(trifluoromethanesulfonyl)imide [emim][NTf_2], but the rate of the Mn^{2+}/Mn^{3+} reaction increased when Au electrodes were used.

The authors also observed that V^{2+}/V^{3+}, V^{3+}/V^{4+} and V^{4+}/V^{5+} redox couples were quasi-reversible in 1-ethyl-3-methylimidazolium bis(trifluoromethanesulfonyl)imide [emim][NTf_2], by cyclic voltammetry at glassy carbon electrode (with a high columbic efficiency of 72%). Moreover, among the following RTILs studied, namely [bmim][BF_4], [bmim][PF_6], [emim][$N(CN)_2$], and [emim][$EtSO_4$], $[EtSO_4]^-$ is the ethylsulfate anion (Figure 8), and only [emim][NTf_2] stabilized the various V^{n+} species (Figure 8A) [42]. In fact, in Figure 8A, we can see clearly three well-defined redox couples centred at −1.37, 0.63, and 0.90 V corresponding to V^{2+}/V^{3+}, V^{3+}/V^{4+} and V^{4+}/V^{5+} oxidations, respectively. Also, the potential difference, ΔE, between the V^{2+}/V^{3+}, V^{3+}/V^{4+} and V^{4+}/V^{5+} couples is 2.0 V, which is comparable to several organic solvents. Such a decrease in ΔE for consecutive redox waves upon changing solvents from acetonitrile to RTILs seems to demonstrate that the RTIL are more basic than most of the common organic solvents. Figures 8B and 8C show that the [$V(acac)_3$] redox couples were not clearly discernible in [bmim][BF_4] and [bmim][PF_6]. In [emim][$N(CN)_2$] and [emim][$EtSO_4$], the redox couple at positive potentials was chemically irreversible (Figures 8D and 8E). Interesting is in the particular case of [emim][$N(CN)_2$], were a cathodic, return peak did appear as the scan rate increased and the ratio of the cathodic to anodic peak currents, also increased. This suggests that a following chemical reaction occurred after oxidation.

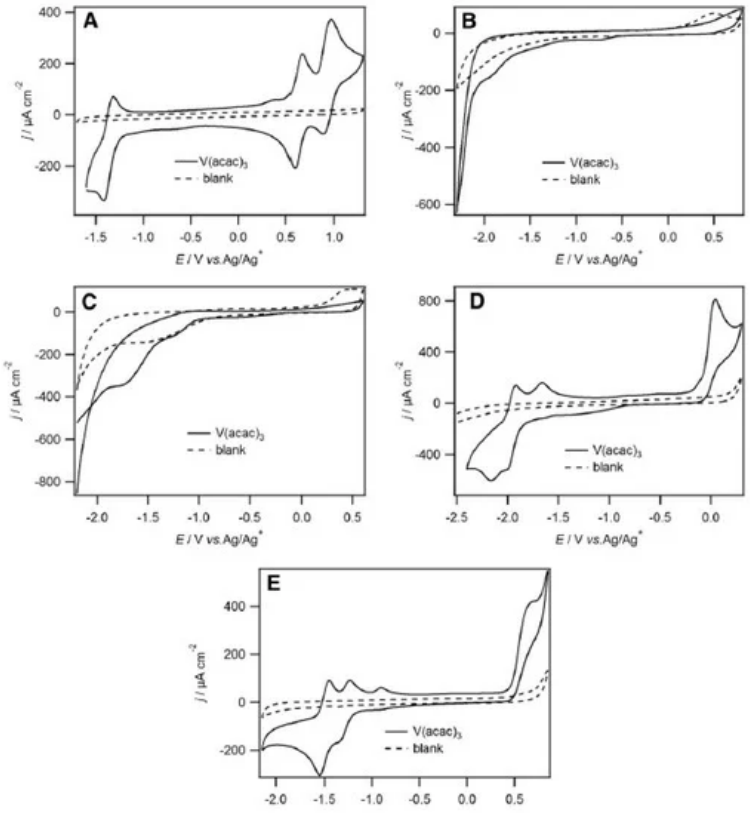

Figure 8. 2nd cycles of cyclic voltammograms recorded at a 5 mm diameter glassy carbon disk electrode at 50 mV/s of (**A**) [$V(acac)_3$] (10 mM) in [emim][NTf_2], (**B**) [$V(acac)_3$] (11 mM) in [bmim][BF_4] (**C**) [$V(acac)_3$] (12 mM) in [bmim][PF_6], (**D**) [$V(acac)_3$] (12 mM) in [emim][$N(CN)_2$] and (**E**) [$V(acac)_3$] (20 mM) in [emim][$EtSO_4$]. All cyclic voltammograms began at

the negative potential limit. Reproduced with permission from [42], copyright 2020, Springer.

In addition, they observed that the use of [bmim][NTf_2] yields almost identical voltammetry to that observed in [[emim][NTf_2], demonstrating that the RTILs anions played the most significant roles in stabilizing the V^{n+} species. They also discussed the importance of diffusion coefficients. The low diffusion coefficients measured, which shown that [emim][NTf_2] are an order of magnitude lower than in acetonitrile, allied with the relatively high viscosity of RTILs can suggest that the RFBs containing [emim][NTf_2] as the electrolyte could face mass transport issues.

Balo et al. [43] applied 1-ethyl-3-methylimidazolium bis(trifluoromethylsulfonyl)imide, [emim][NTf_2], for the recharge of lithium batteries, with promising results. They formed a gel polymer electrolyte (GPE) for high performance lithium polymer batteries (LPBs). The gel is based on the polymer polyethylene oxide and the lithium bis(trifluoromethylsulfonyl)imide salt. By cyclic voltammetric studies, the authors discovered that the gel exhibits promising characteristics suitable for application in LPBs. The GPEs show high thermal stability, high ionic conductivity, high lithium transference number and high electrochemical stability window. One year later, Prasanna and collaborators [44] reported the use of [bmim][NTf_2] incorporated in a polymeric matrix, containing polyvinyl chloride (PVC) and poly(ethyl methacrylate) (PEMA), for the electrochemical study of zinc ion conducting gel polymer electrolytes (GPEs). The prepared films of gel polymer membranes were fully characterized utilizing complex impedance spectroscopy, differential scanning calorimetry thermogravimetric, and cyclic voltammetry analyses. A similar trend was observed for the dielectric constant and ionic conductivity with the increase of [emim][NTf_2] concentration.

Zhang group reported that the use of 1-cyanopropyl-3-methylimidazolium bis(trifluoromethanesulfonyl)imide, [cpmim][NTf_2], as additive in electrolyte for high-voltage lithium-ion batteries (LIBs), sharply increasing the discharge capability of these batteries [45]. Cyclic voltammograms of the $LiNi_{0.5}Mn_{1.5}O_4$/Li system are presented in Figure 9, displaying two redox peaks on each curve.

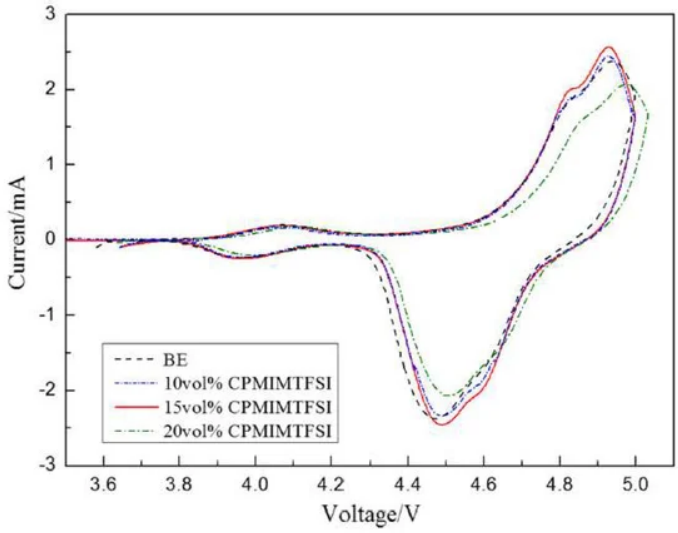

Figure 9. Cyclic voltammograms of $LiNi_{0.5}Mn_{1.5}O_4$/Li cells after 30 cycles with different concentrations of [cpmim][NTf_2] at 0.1 mVs^{-1}. Reproduced with permission from [45], copyright 2020, Springer.

The oxidation peaks were mainly associated to the redox reactions undergone by the transition metals present at $LiNi_{0.5}Mn_{1.5}O_4$/Li. Moreover, the electrolyte with 15 vol.% of [cpmim][NTf_2] had good integrity and large current density. The redox peaks of 20 vol.% of [cpmim][NTf_2] presented lower current intensity than the others, and the oxidation peak was anodically shifted. The authors presented two possible reasons for this shift. One was that the high viscosity of 20 vol.% of [cpmim][NTf_2] increased the internal resistance and the other reason may be related to the high concentration of ionic liquids that led to an enrichment phenomenon on the surface of cathode due to the charge of ionic liquid. As a consequence, the surface structure of the cathode was changed, and thus the peak had a slight shift. Even so, the authors concluded that the mixed electrolyte with [cpmim][NTf_2] is promising to be used in the application of Li-ion batteries.

Recently, the chloroaluminate imidazolium ionic liquid $AlCl_3$/[emim][Cl] was used to test the performance of titanium dioxide (TiO_2) as electrode in rechargeable aluminum-ion batteries. TiO_2 could be a promising electrode material for aluminum-ion battery but it is still quite understudied. Das et al., [46] demonstrate the rechargeability of an Al-ion cell with anatase TiO_2 as cathode in the chloroaluminate ionic liquid electrolyte. The cell of Al-TiO_2 was proven to have an excellent

long-term stability. Also, the electroactive nature of TiO_2 in the chloroaluminate electrolyte was studied both by cyclic voltammetry and galvanostatic cycling studies. The authors observed the existence of a synergistic effect of the current collector in improving the long-term stability of Al-TiO_2 cell.

In the same year, Huang and collaborators [47] also demonstrated that the use of pure 1-ethyl-3-methylimidazolium trifluoromethanesulfonate IL, [emim][OTf], as an ionic liquid electrolyte is a good choice for the design of a dual-graphite battery.

Besides the usage of ILs themselves as electrolytes, some authors have applied them as electrolyte additives. For example, very recently [48], [emim][NTf_2] was studied by cyclic voltammetry for usage as possible additive to the electrolyte in sodium ion batteries Electrochemical cycling of a hard carbon electrode reveals that the $[NTf_2]^-$ anion, mainly coming from the added ionic liquid, can introduce new peaks in the cyclic voltammograms or new steps in the galvanostatic discharge. The products of such degradation can make an interface which determines the cycling properties.

One very interesting work involving the application of ionic liquids as electrolyte additives was developed by Wong et al. [49], who studied the concentration of [emim][BF_4] in an electrolyte to optimize the capacitive performance of high-energy density graphene supercapacitors. The authors reported that the electrolyte viscosity increased exponentially with the increase of IL concentration, while the ionic conductivity decreased with an increase in IL concentration. They also found a strong dependence of the specific capacitance not only on the electrolyte viscosity and ionic conductivity, but also in the maximum working voltage (MWV) where the electrode specific capacitance increases. The neat IL (i.e., [emim][BF_4]) offered the largest specific capacitance and energy density among all IL concentrations for graphene-based electric double-layer capacitors (EDLC), despite having the highest viscosity and the lowest ionic conductivity. The large specific capacitance and energy density was also due to the largest MWV offered by this neat ILs. Another advantage reported by the authors was that, if the EDLC does not require to operate at the electrochemical stability window of the IL, diluted IL electrolytes with an optimized concentration/IL viscosity can be used instead. To sum up, they concluded that the concentration of IL electrolyte should be optimized according to the working voltage required.

[Emim][N(Tf_2)] was also used for studying the electrochemistry of I^-, I_2 and ICl, together with [bmim][Cl], due to the integral role of the I^-/I^{3-} couple in dye-sensitized solar cell technology [50]. Bentley et al., used the cyclic voltammetric technique at a platinum macrodisk electrode in neat ILs, as well as a binary mixture of [bmim]Cl and [emim][N(Tf_2)]. The neutral (I_2) and positive (I^+) oxidation states of iodine are known to have strongly electrophilic behavior, and thus the $I^-/I_2/I^+$ redox processes are sensitive to the presence of nucleophilic chloride or bromide. These anions are both commonly present as impurities in non haloaluminate RTILs. In the absence of chloride (e.g., in neat [emim][N(Tf_2)], I^- was oxidized in an overall one electron per iodide ion process to I_2 via an I_3^- intermediate, gave rise to two resolved I^-/I_3^- and I_3^-/I_2 processes. When Cl^- and I^- were present, even in low concentrations (below 30 mM), an additional oxidation process appears at potentials less positive than the I_3^-/I_2 process. This corresponded, according to the authors, to the oxidation of I_3^- to the inter-halide complex anion $[ICl_2]^-$ in an overall two electrons per iodide ion process.

Also, the electrochemistry of I^-, I_2, and ICl has been investigated by cyclic voltammetry in a binary IL mixture composed of [bmim]Cl and [emim][NTf_2], using the same experimental conditions. The authors studied the effect of the presence of a large excess of Cl^- ($[I^-] \approx 10$ mM and $[Cl^-] \approx 3.7$ M) and observed that I^- was oxidized in an overall two electrons per iodide ion process to $[ICl_2]^-$ via an $[I_2Cl]^-$ intermediate. Bentley and coworkers concluded that in the $I^-/I_2/I^+$ processes, in non haloaluminate ILs, a complicated interplay between multiple electron transfer pathways and homogeneous chemical reactions is present, which may not be at equilibrium on the voltametric time scale.

A mixture of the IL [bmim][BF_4] with acetonitrile as electrolyte was used by Lebedeva et al., to investigate the electrochemical behavior of polyaniline composites, and the author proposed a mechanism involving $[bmim]^+$ as protons source [51].

The search for safer and more sustainable operation conditions has been also pursued in areas such as the mitigation of the greenhouse gas carbon dioxide (a major driver of climate change) through its transformation into value-added products. In fact, CO_2 conversion into valuable chemicals would be the most promising way to reduce CO_2 emissions, making it a part of the solution as carbon feedstock. Moreover, such CO_2 transformation would preferably occur in conditions that allow to avoid the use of volatile and toxic solvents or catalysts (according to the growing demand for eco-friendly synthetic methodologies), as well as of any supporting electrolyte (for a very easy workup of the reaction mixture).

Honores et al. [52] used [bmim][BF_4] and [bmim][NTf_2] to study the electrochemical reduction of carbon dioxide in the presence of cyclam Ni^{2+} and Co^{3+} catalysts (Figure 10).

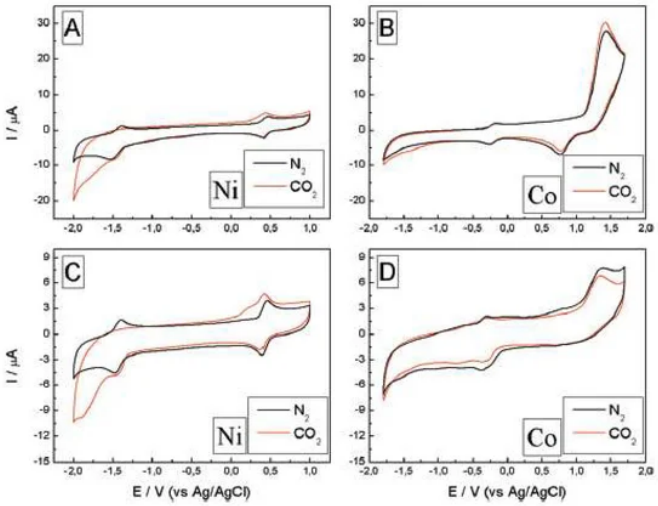

Figure 10. Electrochemical behavior of the system in [bmim][BF_4] (**A**,**B**) and [bmim][NTf_2] (**C**,**D**), [Ni(cyclam)Cl_2] and [Co(cyclam)Cl_2]Cl at 9.7 mM and 2 mM, respectively, both saturated with N_2 (black line) and CO_2 (red line), at 100 mV/s. Reproduced with permission from [52], copyright 2017, Elsevier.

[Ni(cyclam)Cl_2] exhibited a better performance than [Co(cyclam)Cl_3]. Moreover, the solvent had a major impact on the catalytic performance of the systems: the hydrophilic ionic liquid [bmim][BF_4] promoted the catalytic activity, while [bmim][NTf_2] led to very low values of TON.

A study using an ionic liquid bearing the triflate anion, [bmim][OTf], was also used to characterize the cation bismuth/[bmim]$^+$, under conditions for CO_2 reduction [53].

Ratschmeier et al., [54] studied the CO_2 reduction reactions (CO_2RR) at Pt electrodes in four ionic liquids. These electrolytes were 1-ethyl-3-methylimidazolium dicyanamide, [emim][DCA], [emim][BF_4], [bmim][BF_4], and 1-ocytl-3-methylimidazolium tetrafluoroborate, [omim][BF_4]. It was found that water played an important role in CO_2 reduction at a Pt electrode, demonstrating that the formation of an imidazolium carboxylic acid intermediate occurs at electrode potentials of -0,4 V. The authors also reported evidence of the formation of CO. As a consequence, the presence of CO led to deactivation of the Pt surface and to a decrease in reduction currents.

On the other hand, [bmim][NTf_2] was used for the study of adsorption and oxidation of CO. In such work, beyond the CO oxidation, the oxidation of the [NTf_2]$^-$ anion and the release of a proton were observed [55].

The detection of gases has also been explored by cyclic voltammetry in ionic liquids. Yu's group [56] used [bmim][PF_6] for this purpose. They modified this IL with a nickel oxide with reduced graphene oxide to increase the sensitivity to detect O_2.

Huang and collaborators [57] used the functionalized imidazolium IL 1-hydropropyl-3-methylimidazolium tetrafluoroborate, [C_3OHmim][BF_4], for the detection of H_2S. Due to the high absolute values of potential needed to oxidize or reduce H_2S, monoethanolamine (MEA) was added to facilitate its detection (Figure 11).

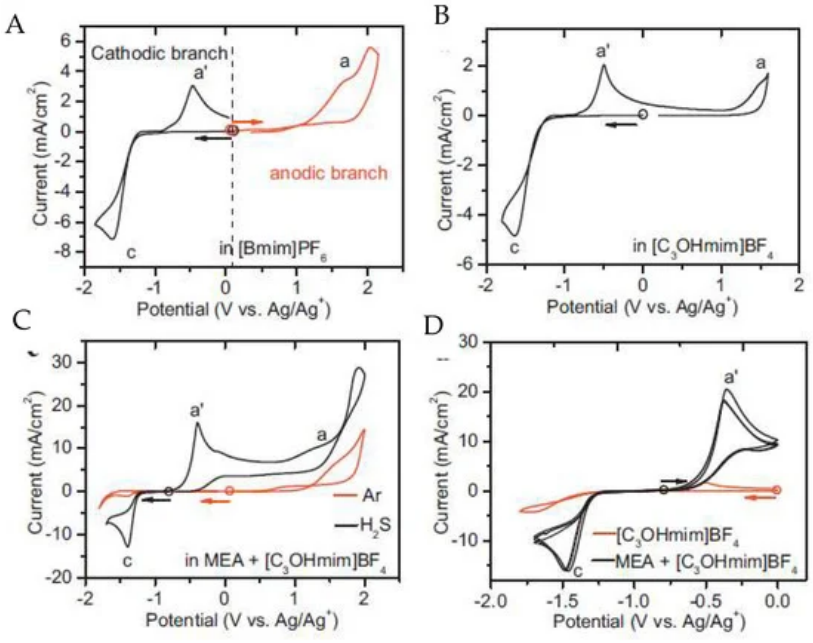

Figure 11. Cyclic voltammograms of H_2S at the Pt microdisk electrode (diameter = 100 µm) in different electrolytes. **A** is [bmim][BF_4]; **B** is [C_3OHmim][BF_4]; **C** is [C_3OHmim][BF_4] with MEA and atmospheric gases and **D** is a comparison of cyclovoltamograms between [C_3OHmim][BF_4] and [C_3OHmim][BF_4] with MEA. Scan rate: 50 mV s^{-1}; the circle indicates the open cell potential (OCP) of each system, and the arrow indicates the start direction of the potential scan from OCP. Reproduced with permission from [57], copyright 2018, Elsevier.

In both [bmim][BF_4] (Figure 11A) and [C_3OHmim][BF_4] (Figure 11B) media, the oxidation/reduction of H_2S occurred at a very high/low potential, close to the upper/lower limit of the electrochemical window of the RTILs. This behaviour led to the conclusion that they were unsuitable for H_2S sensing. Moreover, the addition of MEA to [C_3OHmim][BF_4] electrolyte (Figure 11D increases the solubility of H_2S through chemical absorption, releasing electroactive HS-ions, which subsequently led to an additional anodic response at a potential appropriate for the detection of H_2S. As a final remark, in this study it was possible to conclude that the detection is not affected by ambient gases such as CO_2 or SO_2.

Recently, other functionalized imidazolium ILs were applied in electrochemistry. For example, 1-(2′,3′-dihydroxypropyl)-3-methylimidazolium hydroxide, [dhpmim][OH], provided a good capacitance to nickel oxide nanosheets as electrodes [58]. Further, the electrochemical stability windows of a series of sulfonic-functionalized ILs with trifluoroacetate anion in molecular solvents were investigated, presenting wide potential windows in acetonitrile [59].

In a completely different research area, the electrochemical behaviour of the nucleobases thymine and thymidine was investigated in [bmim][BF_4], observing one- and two-electron reduction peaks, respectively [60], as it is shown in Figure 12. The chronoamperometric fit and the cyclic voltammetry at different scan rates confirmed an irreversible one-electron transfer in both thymine and thymidine.

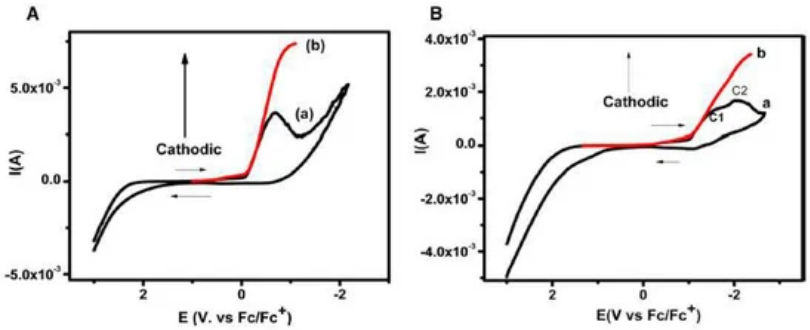

Figure 12. (**A**) Cyclic voltammogram of 5 M thymine at 400 mV/s in [bmim][BF_4] depicting; (**a**) original cyclic voltammogram, (**b**) convoluted cyclic voltammogram. (**B**) Cyclic voltammogram recorded at 400 mV s−1 for 5 mM thymidine in [bmim][BF_4], (**a**) original (**b**) convoluted. Reproduced with permission from [60], copyright 2019, Elsevier.

The corrected cyclic voltammogram of thymine in [bmim][BF_4] at 400 mV s^{-1} (Figure 12A), exhibits the reduction peak at −0.67 V vs. Fc/Fc^+ redox couple. The authors were able to elucidate the electrochemical reductive mechanism involved in the reduction of thymine and thymidine in [bmim][BF_4] by convolutive semi-integral analysis of the cyclic voltametric data produced. The electrochemical reduction of thymine followed a one-electron transfer at the electrode surface resulting in the formation of electron adducts of thymine at the cathode peak. This mechanism is supported by theoretical simulations of the variation of bond dissociation free energy via the concerted sticky dissociative model [60].

From the examples presented above, it is clear that imidazolium based ILs are very promising electrochemical electrolyte media, mainly due to their electrochemical stability and versatility for numerous applications.

References

1. Sustainable Finance: High-Level Conference Kicks EU’s Strategy for Greener and Cleaner Economy into High Gear. A vailable online: https://ec.europa.eu/clima/news/sustainable-finance-high-level-conference-kicks-eus-strategy-greener-and-cleaner-economy-high_en (accessed on 7 November 2020).
2. Climate Strategies & Targets, 2050 Long-Term Strategy. Available online: https://ec.europa.eu/clima/policies/strategies/2050_en (accessed on 7 November 2020).
3. Song, M.H.; Pham, T.P.T.; Yun, Y.S. Ionic liquid-assisted cellulose coating of chitosan hydrogel beads and their applicati on as drug carriers. Rep. 2020, 10, 13905, doi:10.1038/s41598-020-70900-7.
4. Lei, Z.; Chen, B.; Koo, Y.M.; MacFarlane, D.R. Introduction: Ionic liquids. Rev. 2017, 117, 6633–6635, doi:10.1021/acs.chemrev.7b00246.

5. Singh, S.K.; Savoy, A.W. Ionic liquids synthesis and applications: An overview. Mol. Liq. 2020, 297, 112038.
6. Armand, M.; Endres, F.; MacFarlane, D.R.; Ohno, H.; Scrosati, B. Ionic-liquid materials for the electrochemical challeng es of the future. Mater. 2009, 8, 621–629, doi:10.1038/nmat2448.
7. Frontana-Uribe, B.A.; Little, R.D.; Ibanez, J.G.; Palma, A.; Vasquez-Medrano, R. Organic electrosynthesis: A promising green methodology in organic chemistry. Green Chem. 2010, 12, 2099–2119, doi:10.1039/c0gc00382d.
8. Weingarth, D.; Czekaj, I.; Fei, Z.; Foelske-Schmitz, A.; Dyson, P.J.; Wokaun, A.; Koetz, R. Electrochemical stability of i midazolium based ionic liquids containing cyano groups in the anion: A cyclic voltammetry, XPS and DFT study. Electro chem. Soc. 2012, 159, H611–H615, doi:10.1149/2.001207jes.
9. Rupp, A.B.; Krossing, I. Ionic Liquids with Weakly Coordinating [MIII(ORF)4]− Acc. Chem. Res. 2015, 48, 2537–2546, d oi:10.1021/acs.accounts.5b00247.
10. Zhang, S.Y.; Zhuang, Q.; Zhang, M.; Wang, H.; Gao, Z.; Sun, J.K.; Yuan, J. Poly (ionic liquid) composites. Soc. Rev. 20 20, 49, 1726–1755, doi:10.1039/C8CS00938D.
11. DuVall, S.H.; McCreery, R.L. Control of catechol and hydroquinone electron-transfer kinetics on native and modified gla ssy carbon electrodes. Chem. 1999, 71, 4594–4602, doi:10.1021/ac990399d.
12. Miller, J.R.; Simon, P. Electrochemical capacitors for energy management. Mag. 2008, 321, 651–652, doi:10.1126/scie nce.1158736.
13. Kühnel, R.S.; Reber, D.; Remhof, A.; Figi, R.; Bleiner, D.; Battaglia, C. “Water-in-salt” electrolytes enable the use of cos t-effective aluminum current collectors for aqueous high-voltage batteries. Commun. 2016, 52, 10435–10438, doi:10.10 39/C6CC03969C.
14. Ruch, P.W.; Cericola, D.; Foelske, A.; Kötz, R.; Wokaun, A. A comparison of the aging of electrochemical double layer c apacitors with acetonitrile and propylene carbonate-based electrolytes at elevated voltages. Acta 2010, 55, 2352–2357, doi:10.1016/j.electacta.2009.11.098.
15. Tsunashima, K.; Sugiya, M. Electrochemical behavior of lithium in room-temperature phosphonium ionic liquids as lithiu m battery electrolytes. Solid State Lett. 2007, 11, A17–A19, doi:10.1149/1.2820443.
16. Pauliukaite, R.; Doherty, A.P.; Murnaghan, K.D.; Brett, C.M. Characterisation and application of carbon film electrodes i n room temperature ionic liquid media. Electroanal. Chem. 2008, 616, 14–26, doi:10.1016/j.jelechem.2007.12.019.
17. Mohammad, A. Green Solvents II: Properties and Applications of Ionic Liquids; Springer Science & Business Media: Lo ndon, UK, 2012; Volume 2, p. 506.
18. Yuan, W.L.; Yang, X.; He, L.; Xue, Y.; Qin, S.; Tao, G.H. Viscosity, conductivity, and electrochemical property of dicyana mide ionic liquids. Chem. 2018, 6, 59, doi:10.3389/fchem.2018.00059.
19. Kathiresan, M.; Velayutham, D. Ionic liquids as an electrolyte for the electro synthesis of organic compounds. Commun. 2015, 51, 17499–17516, doi:10.1039/C5CC06961K.
20. Largeot, C.; Taberna, P.L.; Gogotsi, Y.; Simon, P. Microporous carbon-based electrical double layer capacitor operating at high temperature in ionic liquid electrolyte. Solid State Lett. 2011, 14, A174–A176, doi:10.1149/2.013112esl.
21. Jaramillo, M.M.; Mendoza, A.; Vaquero, S.; Anderson, M.; Palma, J.; Marcilla, R. Role of textural properties and surface functionalities of selected carbons on the electrochemical behaviour of ionic liquid based-supercapacitors. RSC Adv. 20 12, 2, 8439–8446, doi:10.1039/C2RA21035E.
22. Wei, L.; Yushin, G. Electrical double layer capacitors with sucrose derived carbon electrodes in ionic liquid electrolytes. Power Sources 2011, 196, 4072–4079, doi:10.1016/j.jpowsour.2010.12.085.
23. Elvington, M.C.; Brewer, K.J. Electrochemistry. In Encyclopedia of Inorganic and Bioinorganic Chemistry; John Wiley & Sons: Blacksburg, VA, USA, 2011; pp. 1–22, doi:10.1002/9781119951438.eibc0309.
24. Ibrahim, M.A.M.; Messali, M. Ionic liquid [BMPy]Br as an effective additive during zinc electrodeposition from an aqueo us sulfate bath. Finish 2011, 76, 14.
25. Liu, Y.; Shi, L.; Wang, M.; Li, Z.; Liu, H.; Li, J. A novel room temperature ionic liquid sol-gel matrix for amperometric bios ensor application. Green Chem. 2005, 7, 655–658, doi:10.1039/b504689k.
26. Frackowiak, E.; Lota, G.; Pernak, J. Room-temperature phosphonium ionic liquids for supercapacitor application. Phys. Lett. 2005, 86, 164104, doi:10.1063/1.1906320.
27. Balducci, A.; Dugas, R.; Taberna, P.L.; Simon, P.; Plée, D.; Mastragostino, M.; Passerini, S.J. High temperature carbon-carbon supercapacitor using ionic liquid as electrolyte. Power Sources 2007, 165, 922–927, doi:10.1016/j.jpowsour.200 6.12.048.

28. Bansal, D.; Cassel, F.; Croce, F.; Hendrickson, M.; Plichta, E.; Salomon, M.J. Conductivities and transport properties of gelled electrolytes with and without an ionic liquid for Li and Li-ion batteries. Phys. Chem. B 2005, 109, 4492–4496, doi:10.1021/jp0443963.

29. Lee, S.-Y.; Yong, H.H.; Lee, Y.J.; Kim, S.K.; Ahn, S. Two-cation competition in ionic-liquid-modified electrolytes for lithium ion batteries Phys. Chem. B 2005, 109, 13663–13667, doi:10.1021/jp051974m.

30. Fredin, K.; Gorlov, M.; Pettersson, H.; Hagfeldt, A.; Kloo, L.; Boschloo, G. On the influence of anions in binary ionic liquid electrolytes for monolithic dye-sensitized solar cells. Phys. Chem. C 2007, 111, 13261–13266, doi:10.1021/jp072514r.

31. Pinilla, C.; Del Popolo, M.G.; Lynden-Bell, R.M.; Kohanoff, J. Structure and dynamics of a confined ionic liquid. topics of relevance to dye-sensitized solar cells. Phys. Chem. B 2005, 109, 17922–17927, doi:10.1021/jp052999o.

32. Caporali, S.; Marcantelli, P.; Chiappe, C.; Pomelli, C.S. Electrodeposition of transition metals from highly concentrated solutions of ionic liquids. Coat. Technol. 2015, 264, 23–31, doi:10.1016/j.surfcoat.2015.01.031.

33. Barrado, E.; Rodriguez, J.A.; Hernández, P.; Castrillejo, Y. Electrochemical behavior of copper species in the 1-buthyl-3-methyl-imidazolium chloride (BMIMCl) ionic liquid on a Pt electrode. Electroanal. Chem. 2016, 768, 89–101, doi:10.1016/j.jelechem.2016.02.034.

34. Gupta, R.; Gupta, S.K.; Gamre, J.S.; Lohithakshan, K.V.; Natarajan, V.; Aggarwal, S.K. Understanding the dynamics of Eu3+ ions in room-temperature ionic liquids—Electrochemical and time-resolved fluorescence spectroscopy studies. J. Inorg. Chem. 2015, 104–111, doi:10.1002/ejic.201402713.

35. Rama, R.; Rout. A.; Venkatesan, K.A.; Antony, M.P.; Rao, P.R.V. Electrochemical behavior of Eu(III) in imidazolium ionic liquid containing tri-n-butyl phosphate and N,N-dihexyloctanamide ligands. Electroanal. Chem. 2015, 757, 36–43, doi:10.1016/j.jelechem.2015.09.005.

36. Krishna, G.M.; Rout, A.; Venkatesan, K.A. Voltammetric investigation of some lanthanides in neutral ligand-ionic liquid. Electroanal. Chem. 2020, 856, 113671, doi:10.1016/j.jelechem.2019.113671.

37. Sengupta, A.; Murali, M.S.; Mohapatra, P.K.; Iqbal, M.; Huskens, J.; Verboom, W. Extracted species of Np(IV) complex with diglycolamide functionalized task specific ionic liquid: Diffusion, kinetics and thermodynamics by cyclic voltammetry. Radioanal. Nucl. Chem. 2015, 304, 563–570, doi:10.1007/s10967-014-3857-8.

38. Sengupta, A.; Murali, M.S.; Mohapatra, P.K.; Iqbal, M.; Huskens, J.; Verboom, W. Np(IV) complex with task-specific ionic liquid based on CMPO: First cyclic voltammetric study. Chem. 2015, 146, 1815–1821, doi:10.1007/s00706-015-1467-y.

39. Rama, R.; Rout. A.; Venkatesan, K.A.; Antony, M.P. Effect of alkyl chain length of tri-n-alkyl phosphate extractants on the electrochemical behaviour of U(VI) in ionic liquid medium. Electroanal. Chem. 2016, 771, 87–93, doi:10.1016/j.jelechem.2016.04.001.

40. Krishna, G.M.; Suneesh, A.S.; Kumaresan, R.; Venkatesan, K.A.; Antony, M.P. Electrochemical behavior of U(VI) in imidazolium ionic liquid medium containing tri-n-butyl phosphate and chloride ion and spectroscopic characterization of uranyl species. ChemistrySelect 2017, 2, 8706–8715, doi:10.1002/slct.201701139.

41. Krishna, G.M.; Venkatesan, K.A. Coordination and electrochemical behavior of U(VI) in dicyanamide ionic liquid. Spectrosc. 2019, 103, 102927, doi:10.1016/j.vibspec.2019.102927.

42. Ejigu, A.; Greatorex-Davies, P.A.; Walsh, D.A. Room temperature ionic liquid electrolytes for redox flow batteries. Commun. 2015, 54, 55–59, doi:10.1016/j.elecom.2015.01.016.

43. Balo, L.; Shalu; Gupta, H.; Singh, V.K.; Singh, R.K. Flexible gel polymer electrolyte based on ionic liquid EMIMTFSI for rechargeable battery application. Acta 2017, 230, 123–131, doi:10.1016/j.electacta.2017.01.177.

44. Prasanna, C.M.S.; Suthanthiraraj, S.A. Dielectric and thermal features of zinc ion conducting gel polymer electrolytes (GPEs) containing PVC / PEMA blend and EMIMTFSI ionic liquid. Ionics 2018, 24, 2631–2646, doi:10.1007/s11581-017-2421-2.

45. Zhang, W.; Wang, Y.; Lan, X.; Huo, Y. Imidazolium-based ionic liquids as electrolyte additives for high-voltage Li-ion batteries. Chem. Intermed. 2020, 46, 3007–3023, doi:10.1007/s11164-020-04128-5.

46. Das, S.K.; Palaniselvam, T.; Adelhelm, P. Electrochemical study on the rechargeability of TiO2 as electrode material for Al-ion batteries with chloroaluminate ionic liquid electrolyte. Solid State Ion. 2019, 340, 115017, doi:10.1016/j.ssi.2019.115017.

47. Huang, Y.; Xiao, R.; Ma, Z.; Zhu, W. Developing dual-graphite batteries with pure 1-ethyl-3-methylimidazolium trifluoromethanesulfonate ionic liquid as the electrolyte. ChemElectroChem 2019, 6, 4681–4688, doi:10.1002/celc.201901171.

48. Benchakar, M.; Naéjus, R.; Damas, C.; Santos-Peña, J. Exploring the use of EMImFSI ionic liquid as additive or co-solvent for room temperature sodium ion battery electrolytes. Acta 2020, 330, 135193, doi:10.1016/j.electacta.2019.135193.
49. Wong, S.I.; Lin, H.; Sunarso, J.; Wong, B.T.; Jia, B. Optimization of ionic-liquid based electrolyte concentration for high-energydensity graphene supercapacitors. Mat. Today 2020, 18, 100522, doi:10.1016/j.apmt.2019.100522.
50. Bentley, C.L.; Bond, A.M.; Hollenkamp, A.F.; Mahon, P.J.; Zhang, J. Electrochemistry of iodide, iodine, and iodine monochloride in chloride containing nonhaloaluminate ionic liquids. Chem. 2016, 88, 1915–1921, doi:10.1021/acs.analchem.5b04332.
51. Lebedeva, M.V.; Gribov, E.N. Electrochemical behavior and structure evolution of polyaniline/carbon composites in ionic liquid electrolyte. Solid State Electrochem. 2020, 24, 739–751, doi:10.1007/s10008-020-04516-2.
52. Honores, J.; Quezada, D.; García, M.; Calfumán, K.; Muena, J.P.; Aguirre, M.J.; Arévalo, M.C.; Isaacs, M. Carbon neutral electrochemical conversion of carbon dioxide mediated by [Mn+(cyclam)Cln] (M = Ni2+ and Co3+) on mercury free electrodes and ionic liquids as reaction media. Green Chem. 2017, 19, 1155–1162, doi:10.1039/c6gc02599d.
53. Medina-Ramos, J.; Zhang, W.; Yoon, K.; Bai, P.; Chemburkar, A.; Tang, W.; Atifi, A.; Lee, S.S.; Fister, T.T.; Ingram, B.J.; et al. Cathodic corrosion at the bismuth−ionic liquid electrolyte interface under conditions for CO2 Chem. Mater. 2018, 30, 2362–2373, doi:10.1021/acs.chemmater.8b00050.
54. Ratschmeier, B.; Kemna, A.; Braunschweig, B. Role of H2O for CO2 reduction reactions at platinum/electrolyte interfaces in imidazolium room-temperature ionic liquids. ChemElectroChem 2020, 7, 1765–1774, doi:10.1002/celc.202000316.
55. Tang, Y.; Liu, X.; McMahan, J.; Kumar, A.; Khan, A.; Sevilla, M.; Zeng, X. Adsorption and electrochemistry of carbon monoxide at the ionic liquid−Pt interface. Phys. Chem. B 2019, 123, 4726–4734, doi:10.1021/acs.jpcb.8b11602.
56. Yu, L.; Liu, J.; Yin, W.; Yu, J.; Chen, R.; Song, D.; Liu, Q.; Li, R.; Wang, J. Ionic liquid combined with NiCo2O4/rGO enhances electrochemical oxygen sensing. Talanta 2020, 209, 120515, doi:10.1016/j.talanta.2019.120515.
57. Huang, Q.; Li, W.; Wu, T.; Ma, X.; Jiang, K.; Jin, X. Monoethanolamine-enabled electrochemical detection of H2S in a hydroxylfunctionalized ionic liquid. Commun. 2018, 88, 93–96, doi:10.1016/j.elecom.2017.12.024.
58. Bhise, S.C.; Awale, D.V.; Vadiyar, M.M.; Patil, S.K.; Ghorpade, U.V.; Kokare, B.N.; Kim, J.H.; Kolekar, S.S. A mesoporous nickel oxide nanosheet as an electrode material for supercapacitor application using the 1-(2_,3_-dihydroxypropyl)-3-methylimidazolium hydroxide ionic liquid electrolyte. Mater. Sci. 2019, 42, 263, doi:10.1007/s12034-019-1961-7.
59. Das, S.; Dutta, T.; Borah, R. Comparative study of the physical and electrochemical behavior of direct N-SO3H functionalized 1, 3-disulfo-2-alkyl imidazolium trifluoroacetate ionic liquids in molecular solvents. Mol. Liq. 2019, 289, 111099, doi:10.1016/j.molliq.2019.111099.
60. Tayade, S.; Patil, K.; Sharma, G.; Patil, P.; Mane, R.M.; Mahulikar, P.; Sharma, K.K.K. Electrochemical investigations of thymine and thymidine in 1-butyl-3-methyl imidazolium tetrafluoroborate ionic liquids at room temperature. Pap. 2019, 73, 2275–2282, doi:10.1007/s11696-019-00777-y.